LIMNOLOGY and OCEANOGRAPHY

ASLO

Limnol. Oceanogr. 9999, 2025, 1–14

doi: 10.1002/lno.70024

RESEARCH ARTICLE

Dynamics of surface accretion and surface elevation differ between river and tide dominated settings in tropical mangroves

Catherine E. Lovelock[1*] **Marilyn C. Ball**[2] **Nigel Brothers**[1] **Alex Pearse**[1] **Ruth Reef**[3]

[1]School of the Environment, The University of Queensland, St Lucia, Queensland, Australia; [2]Research School of Biology, Australian National University, Acton, Australian Capital Territory, Australia; [3]School of Earth Atmosphere and Environment, Monash University, Clayton, Victoria, Australia

Abstract

The maintenance of soil surface elevation in mangroves supports the persistence of mangroves with sea level rise. The processes contributing to soil surface elevation have rarely been assessed in the humid tropics, despite most mangroves occurring in river deltas and tidal estuaries within this climate zone. Using surface elevation table (SET) with marker horizon methods over sites that occurred on either the main river channel or a tidal channel, we assessed the role of rainfall and associated river discharge in moderating surface elevation in mangroves of the Daintree River, Queensland, Australia. In the sites in the main river channel close to the river mouth, increases in soil surface elevation were episodic, with river flooding leading to greater accretion of sediment and increases in surface elevation in years with high river discharge, while in the tidal channel further from the mouth, sediment accretion and surface elevation increments were variable among years and not linked to river discharge. Our study finds that the 32.7 km^2 of mangroves of the Daintree River estuary have surface elevation gains that are variable but similar to current rates of sea level rise through trapping of around 40,000 t of sediment annually, mainly within the downstream mangroves and those in the main river channel. Extreme rainfall and river flows have spatially variable influences on surface elevation in mangroves of the Daintree River, which may lead to similarly variable responses to accelerating sea level rise.

Mangroves are vulnerable to land-use change, sea level rise and other climate change factors (Goldberg et al. 2020; Saintilan et al. 2020; Friess et al. 2022). Mangroves are important for the ecosystem services they provide which includes carbon sequestration, coastal protection, fisheries and biodiversity and water quality improvement through trapping sediments and cycling nutrients (Barbier 2017). Key to mangrove persistence in the landscape over the long-term (decades, centuries to millennia) is the maintenance of their position in the intertidal zone relative to sea level through increased elevation of the soils surface. Increases in surface elevation of mangroves can thereby avoid levels of inundation that exceed tree species physiological tolerance of flooding that may result in changes in mangrove species composition and structure and potential loss of mangroves to open water (Friess et al. 2022).

Changes in soil surface elevation (vertical adjustment of the soil surface) measured using surface elevation tables (SETs) are influenced by a range of interacting surface and subsurface processes (Cahoon 2024). Sediments delivered during tidal inundation of mangroves maintain and increase surface elevation in many mangrove environments, but subsurface root growth and other organic matter inputs (e.g., woody debris and algal biofilms) can also be important for maintaining soil surface elevation (McKee et al. 2007; McKee 2011; Krauss et al. 2014). Declines in surface elevation that lead to increases in the relative rate of sea level rise in wetlands can be caused by erosion of surface sediments and shallow subsidence due to compaction of the soil profile (Rogers and Saintilan 2021). Compaction can occur with decomposition of roots and soil organic matter, with mortality of the vegetation, shrinkage of the soil profile

*Correspondence: c.lovelock@uq.edu.au

Associate editor: Anna Armitage

Data Availability Statement: All data is available within the published manuscript.

associated with declines in groundwater, and compression of the soil pore space linked to the mass of overlying tidal water and sediments, called overburden (Rogers and Saintilan 2021; Cahoon 2024).

While the processes that influence mangrove soil surface elevation are broadly known (Krauss et al. 2014; Cahoon 2024), there are gaps in knowledge of the relative importance of processes contributing to surface elevation in tropical mangrove ecosystems. Changes in surface elevation may vary among climatic and geomorphic settings, and land uses (Sasmito et al. 2016). Among geomorphic settings, varying exposure to freshwater river flows, waves, and tides can influence surface and subsurface processes that determine mangrove surface elevation (Woodroffe et al. 2016). In river deltas, rivers discharge sediments and nutrients eroded from catchments downstream. As rivers widen toward the mouth and rates of water flow decline, sediments are deposited in fringing wetlands during tidal inundation that increases their elevation (McLachlan et al. 2020). Additionally, nutrients are delivered to mangroves in river flows and in groundwater, which, along with low salinity, enhances mangrove productivity that can contribute to subsurface expansion through root growth (McKee 2011; Krauss et al. 2014). Extreme events like floods intermittently decrease salinity and increase sediment and nutrient availability due to greater catchment runoff, enhancing surface elevation in depocenters, although this was spatially variable (Hensel et al. 1999; Sasmito et al. 2016; Feher et al. 2020).

The influence of tides in river deltas creates complexity in sediment dynamics but tends to stabilize the morphology of deltas (Hoitink et al. 2017). The stability of tidal dominated systems indicates that the import and export of sediments in tidal flows may be more balanced compared to river dominated systems (Hoitink et al. 2017) which may lead to lower levels of sediment accretion and lower delivery of nutrients (attached to sediment particles) resulting in less favorable conditions for mangrove growth and lower levels of surface elevation increments in mangroves of tidal dominated systems compared to those in mangroves fringing river channels (McLachlan et al. 2020). Finally, shallow groundwater on coasts varies with rainfall, water extraction, and catchment characteristics and can influence rates of wetland soil subsidence that may differ among sites and geomorphic settings (Whelan et al. 2005). Differences in sediment accretion, nutrient availability, salinity, groundwater, and mangrove productivity between river and tide dominated systems may therefore lead to higher levels of surface elevation gains in river dominated mangroves compared to tide dominated mangroves due to higher levels of sediment accretion and root growth, although differences in surface elevation increments between geomorphic settings may be moderated by processes leading to soil compaction (Rogers and Saintilan 2021; Cahoon 2024).

The Daintree River in the humid tropical region of the Great Barrier Reef coast has a large, diverse, mangrove-rich estuary (Bunt et al. 1982). Tall mangroves, dominated by *Rhizophora apiculata* and *Bruguiera* spp., occur along the main channel of the river (high connectivity channel, sensu McLachlan et al. 2020). Mangroves also form extensive forests along the sinuous tidal channel of the South Arm that terminates in a dead end (low connectivity channel) (Held et al. 2003; Fig. 1). The South Arm fringing mangroves are variable in stature and include *Bruguiera* spp., *Xylocarpus* spp., *Rhizophora stylosa*, *Lumnitzera* spp., and *Ceriops* spp. (Held et al. 2003). We used the variation in the geomorphic setting of the mangroves of the Daintree River estuary as a natural experiment to assess the relative importance of sediment accretion, root growth, and other processes that influence surface elevation increments, comparing sites on the main channel of the river to sites in the tide-dominated South Arm. We anticipated that (1) sediment accretion and its contributions to mangrove surface elevation in the main channel would be greater than those in the tidal channel; (2) sediment accretion and surface elevation gains would be higher closer to the river mouth than upstream; and (3) root growth contributions to surface elevation gains would be higher in the main channel than in the tidal channel, reflecting differences in mangrove structural development and productivity.

In this tropical humid region of Australia, interannual variation in rainfall is high and strongly influenced by El Niño Southern Oscillation (ENSO) cycles (Lough 1994; Sharmila and Hendon 2020). In La Niña phases, high levels of rainfall lead to flooding, erosion of sediments from the catchments, and large fluxes of sediments in river flows to coastal waters (Bartley et al. 2018). We therefore anticipated that changes in surface elevation in the Daintree River mangroves would be sensitive to the magnitude of rainfall and resulting river flows because sediment supply is increased as sediments are mobilized from the catchment during high rainfall events (Leonard and Nott 2015; Croke et al. 2017).

Materials and methods

Site description

The Daintree River in northern Queensland (Lat. 16°220S; Long. 145°250E) lies within the World Heritage Area of the Great Barrier Reef and has a catchment area of 2107 km^2. The catchment is relatively undisturbed and is mostly covered in tropical rainforest, with limited areas of sugarcane, grazing, and urban development (only 0.1% of the catchment area is highly modified, Davies and Eyre 2005). Thus, sediment delivery to the ocean after European colonization was estimated as 1.2 times pre-European levels (McCloskey et al. 2021), while sediment runoff in more modified catchments is estimated to be, on average, 3.7–5.5 times greater than fluxes prior to European colonization (Kroon et al. 2012; McCloskey et al. 2021).

The Daintree River system is classified as a tide-dominated delta (Harris et al. 2002). Mean annual rainfall in the region is 2037 mm yr^{-1} (Australian Bureau of Meteorology). Although rainfall is highest in the wet season (November–February), rain

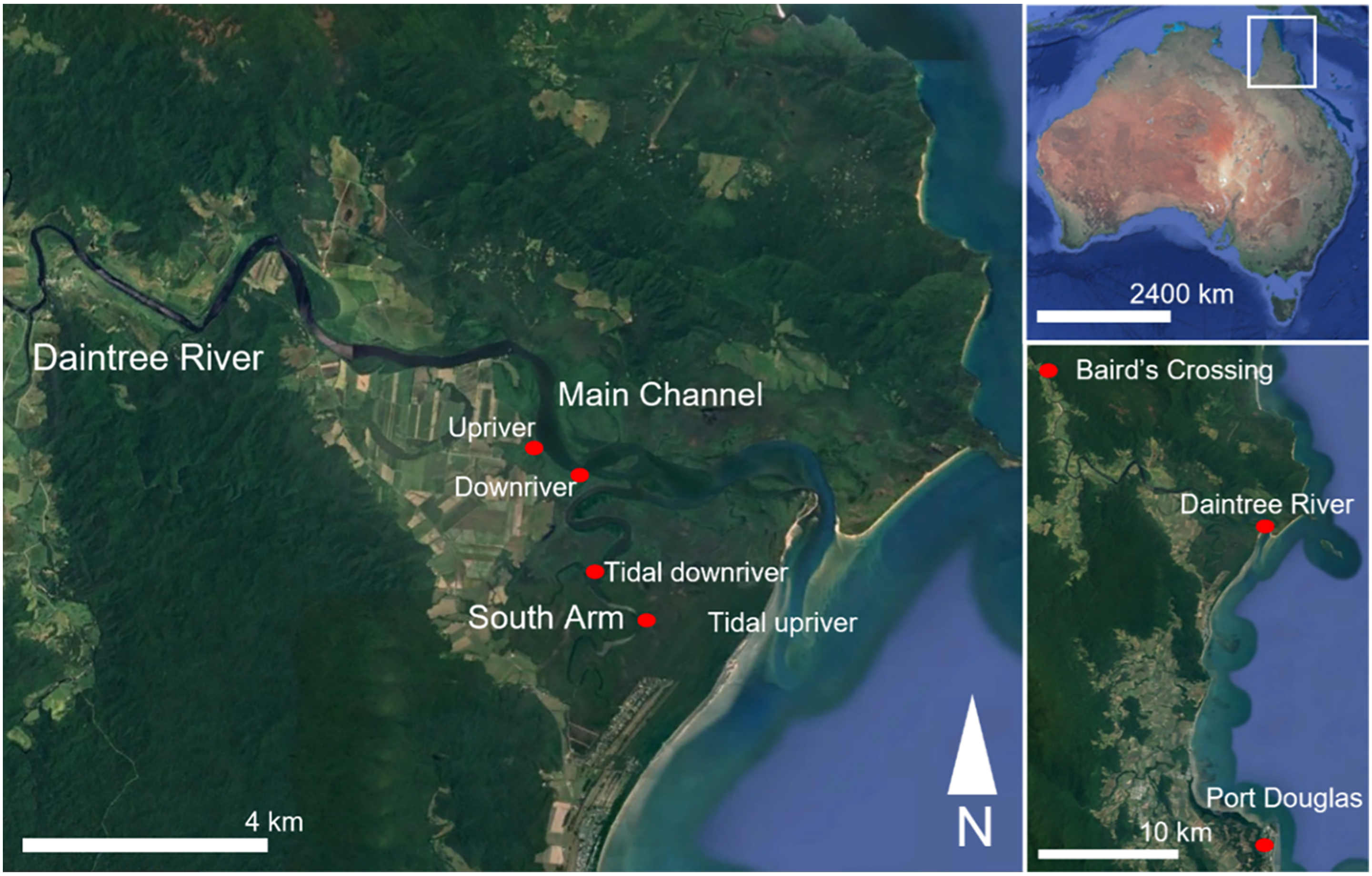

Fig. 1. Map of the study site and location of the surface elevation tables. Inset shows the region at a larger scale and the location of the river flow monitoring site upstream at Baird's Crossing.

usually occurs in all months, even throughout the dry season (July–October). Mean maximum annual air temperature is 27.9°C, with mean minimum temperatures of 16.8°C in the coolest month (July) and mean maximum temperatures of 30.3°C in December and January. The tides are semidiurnal with a range of 3.35 m.

The intertidal mangroves in the Daintree River estuary are extensive (32.7 km^2) and diverse (28 species; Duke et al. 1998). The mangroves fringe the main channel of the river and occur within a network of tidal creeks, the largest of which is the South Arm (Fig. 1). The mangroves are highly variable in forest composition and structure (Held et al. 2003). They can reach 30 m in height in areas fringing the channels, but there are also extensive scrub mangroves, mostly occurring in the South Arm, that occur between taller fringing vegetation and the landward edges of the mangrove (Held et al. 2003; Lovelock et al. 2017).

Experimental design

Twelve SET-marker horizon instruments (Cahoon et al. 2002) were established in two different geomorphic settings: (1) in the mangroves fringing the main channel of the Daintree River, and (2) fringing the tidal channel of the South Arm. In each geomorphic setting, sites were established at two locations along the river (termed "upriver" and "downriver") (Fig. 1). Three replicate SETs (comprised of stainless-steel rod) with marker horizons were installed at each site between 2014 and 2015, which were then monitored annually (in July or August) to 2022. Measurements using SETs monitor changes in the elevation of the soil surface over time relative to a fixed benchmark (BM) anchored within the soil profile (Cahoon et al. 2002). In this study, benchmarks were 7–12 m deep (Table 1). Threaded stainless steel rods (1.4 cm diameter) were hammered (using a slide hammer) into the sediment to refusal. Sites were selected to be similar in their characteristics to increase the potential of detecting differences in processes between the main channel and tidal channel. They were selected to represent typical mangrove communities of the Daintree River that were similar in elevation and inundation regimes (Table 1). They had similar exposure (on southern banks), in straight sections of the river, and with Upriver and Downriver sites at similar distances to the confluence of the

Table 1. Variation in depth of the surface elevation table benchmark, the elevation of the site above the Australian Height Datum (AHD), the maximum depth of inundation (2015–2016) and the % time inundated for mangrove sites in the main channel of the Daintree River and the tidal channel of the South Arm. The elevation of the sites was obtained from a digital elevation model with a vertical accuracy of 0.8 m and horizontal accuracy of 0.3 m.

Geomorphic setting	Position	Depth of the rod benchmark (m)	Elevation above AHD m (DEM)	Maximum inundation depth (m)	Inundation (% time inundated)	Dominant mangrove species
Main channel, Daintree	Downriver	11.2	1.08	0.75	21	*Rhizophora apiculata*
	Upriver	10.4	1.35	0.48	20	*Bruguiera gymnorrhiza*
Tidal channel, south arm	Downriver	9.6	0.75	0.48	16	*B. gymnorrhiza*
	Upriver	7.3	0.82	0.71	25	*B. gymnorrhiza*

tidal South Arm and main river channel. Finally, sites were accessible by small boat and were safe to access, limiting exposure to estuarine crocodiles.

Elevation of the sites within the intertidal zone was obtained from the digital elevation model available nationally (5 m grid, horizontal accuracy of 0.8 m, vertical accuracy 0.3 m) (Geoscience Australia 2015). Elevation of the sites varied from 0.75 to 1.35 m relative to the Australian Height Datum (AHD) and was 30–50 cm higher in the main channel compared to the tidal channel (Table 1). Comparison of inundation depth and duration of inundation among the sites was assessed in 2015–2016 using water level loggers that recorded water levels every 15 min (Hobo, Onset, MA, USA) and that were attached to the middle SET at each site (Table 1). For 2015–2016, maximum inundation depths varied by 30 cm (from 0.48 to 0.75 m) and the proportion of the time the sites were inundated ranged from 16% to 25% (Table 1).

Monitoring of surface elevation and surface accretion

At each monitoring period, a leveled arm (the table) was placed on the benchmark and the elevation of the surface was determined by lowering nine fiberglass pins to the soil surface in four different directions around the benchmark rod (36 measurements in total) (Cahoon et al. 2002). The height of the fiberglass pins above the arm was measured with a metal ruler.

Adjacent to the SET marker horizons comprised of white feldspar, were deployed on the soil surface to provide a measure of material accumulating on the soil's surface (e.g., sediment and detritus). Because our sites have high levels of bioturbation that limit the durability of feldspar marker horizons, in 2016 we deployed three small concrete tiles (9 × 16 cm, 2 cm thick) buried under the sediment to assess surface accretion (Swales and Lovelock 2020). Although Swales and Lovelock (2020) recommended the use of mesh tiles over solid tiles to avoid altering porewater flow (through compaction) and root growth, we chose to use small solid tiles because limited soil disturbance was required to install them and because of bioturbation by large crabs and mud lobsters that overturned mesh tiles when we trialed this method. Surface accretion rates measured on small tiles and mesh tiles were observed to be similar in the study of Swales and Lovelock (2020). Annually we monitored surface accretion over the tiles using a metal ruler pushed through the accumulated sediment to the tile below (Swales and Lovelock 2020).

Monitoring elevation change in the top 35 cm of the soil profile

To further assess processes occurring in the top 35 cm of the soil that may be contributing to soil surface elevation changes and shallow subsidence, we deployed in 2017 an array of eight 60 cm pins (7 mm diameter) adjacent to each SET. Pins were pushed into the sediment to a depth of 35 cm. No scouring around pins or SETs was observed. High root densities occur in the top 35 cm (Castañeda-Moya et al. 2011; Arnaud et al. 2023) and thus changes in the pin height were assumed to reflect changes in soil volume due to sediment (and organic matter) deposition on the soil surface, root dynamics (growth and decomposition), and compaction of the top layer of soil, similar to data provided by Shallow SETs (Cahoon 2024). We measured the height of the exposed pins at each measurement interval with a ruler.

Calculating rates of surface elevation change and shallow subsidence

For each SET, marker horizon and pins, initial measurements were considered zero and changes in surface elevation, surface accretion, and root zone volume (from pin heights) were plotted over time to provide a visual display of the dynamics of surface elevation and other parameters. For each SET, we assessed trends in surface elevation, surface accretion, and pin height over the 8 yr of the time series using linear regression (*see* Data analyses section). Slopes of the regression lines were called ΔSurface Elevation, ΔSurface Accretion, and ΔPin Height, respectively. From these trends, we calculated ΔShallow subsidence due to compaction of the soil profile over the length of the benchmark (BM) calculated (Cahoon et al. 2002) as:

$$\Delta\text{Shallow Subsidence}_{\text{BM}} = \Delta\text{Surface Accretion} - \Delta\text{Surface Elevation}$$

We then calculated shallow subsidence in the top 35 cm of the soil profile (Shallow $\text{Subsidence}_{35\text{cm}}$) in an analogous way to that used for ΔShallow $\text{subsidence}_{\text{BM}}$ (described above), as

$$\Delta \text{Shallow subsidence}_{35\text{cm}} = \Delta \text{Surface Accretion} - \Delta \text{Pin height}.$$

By convention, positive values of shallow subsidence reflect losses in soil volume, while negative values reflect subsurface processes that increase soil volume (Cahoon et al. 2002).

Root growth and potential contributions to surface elevation

To assess for differences in root growth between geomorphic settings, we used root in-growth bags for 1 yr, between July 2017 and July 2018 (Ola et al. 2018). Root bags were nylon mesh tubes (5.5 cm diameter and 21 cm long) filled with a mix of peat moss and clean river sand, giving a substrate with a dry bulk density of 0.56 g cm^{-3}, which is comparable to soil bulk density for mangroves in the region (Boto and Wellington 1984) and is suitable for root growth (Ola et al. 2018). Root bags were inserted into holes in the soil made with a soil corer of equivalent size to the ingrowth bags (to ~ 20 cm depth) and secured to a nearby stem using monofilament to facilitate retrieval. Five root in-growth bags for each SET station were deployed in July 2017 and retrieved in July 2018 using a knife to cut roots entering the bag before extraction from the soil. Root bags were opened and gently washed over a 1 mm diameter sieve (Castañeda-Moya et al. 2011). All roots that grew within the bags were collected, and the volume of roots assessed (in cm^3) using water volume displacement in a graduated cylinder. Roots were dried to constant weight to determine the dry mass of roots grown in the root bag during the interval.

Assessing interannual variation in surface elevation

Because our study was concerned with the effects of interannual variation in rainfall and river flows, we also calculated annual increments in surface elevation, surface accretion, and pin height for each year of the study as Surface $\text{Elevation}_{\text{ANNUAL}}$, Surface $\text{Accretion}_{\text{ANNUAL}}$, and Pin $\text{Height}_{\text{ANNUAL}}$. We calculated annual shallow subsidence to the benchmark ΔShallow $\text{subsidence}_{\text{BM\_ANNUAL}}$ and in the root zone Shallow $\text{Subsidence}_{35\text{cm\_ANNUAL}}$ in a similar manner as described above.

Annual variation in environmental data

We collated climate and water data from the closest available monitoring stations, including rainfall data from the Daintree Village station (Station 031127, Bureau of Meteorology, Australian Government), river flows from station 108002A Daintree River at Bairds Crossing (https://water-monitoring.information.qld.gov.au/, Queensland Government Water Monitoring, Government of Queensland), and turbidity monitored at the Daintree ferry crossing (2.5 km upstream from the upriver SET site on the main channel) and at the river mouth (https://water-monitoring.information.qld.gov.au/, Queensland Government Water Monitoring, Government of Queensland) (Fig. 2). Turbidity in the river is mainly associated with suspended sediments (Hodge et al. 2005; Davies and Eyre 2005). The local rate of sea level rise was 1.8 mm per yr^{-1} from the Cairns tide gauge (Bureau of Meteorology, http://www.bom.gov.au/ntc/IDO70000/IDO70000_59060_SLD.shtml). An annual mean of each of these data sources were calculated to match the monitoring periods of our SET-MH measurements.

Data analyses

Linear trends (slopes) in surface elevation (ΔSurface elevation), surface accretion on tiles (ΔSurface accretion) and changes in pin height (ΔPin height) data for each SET-MH station were established using linear regression over the years. Using the slopes, we assessed differences in ΔSurface elevation, ΔSurface accretion, ΔShallow $\text{subsidence}_{\text{BM}}$, and ΔShallow $\text{subsidence}_{35\text{cm}}$ between geomorphic settings (main channel Daintree River/tidal channel South Arm) and locations (downriver/upriver) using two-way ANOVA where geomorphic setting (main river channel or tidal channel) and location (downriver/upriver) were fixed factors in the analysis. Root growth data for 2017–2018 were analyzed using a

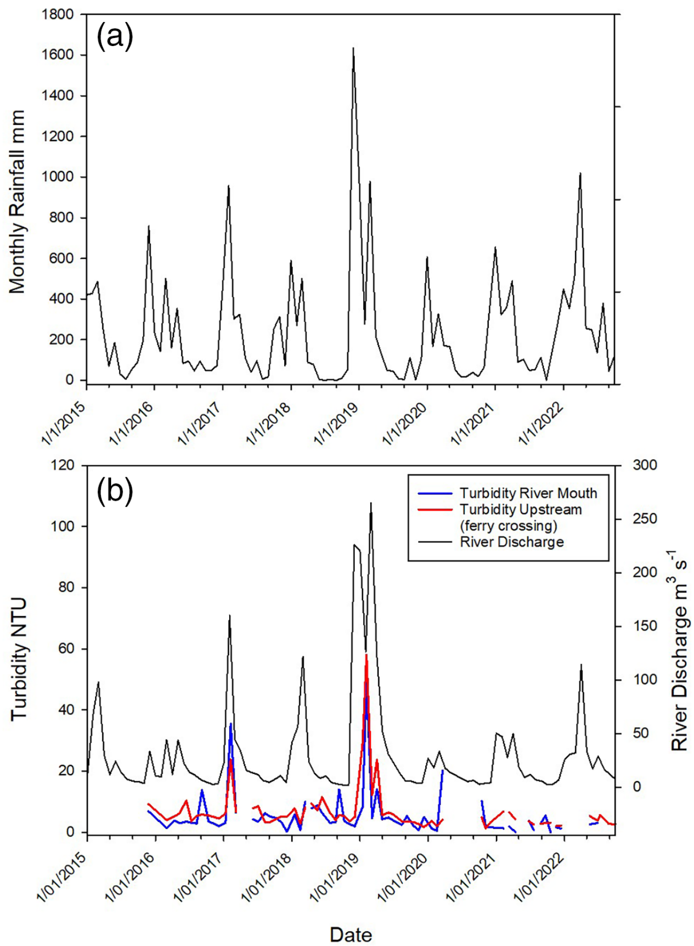

Fig. 2. Rainfall (**a**), river flow, and turbidity (**b**) in the Daintree River over the study period.

similar ANOVA model where geomorphic settings (main channel Daintree River/tidal channel South Arm) and locations (downriver/upriver) were included in the model as fixed factors.

To evaluate the variation in annual increments (Surface Elevation$_{ANNUAL}$, Surface Accretion$_{ANNUAL}$ Pin Height$_{ANNUAL}$, Shallow subsidence$_{BM_ANNUAL}$ and Shallow Subsidence$_{35cm_ANNUAL}$) between geomorphic settings and locations in the estuary, we used repeated measures analysis, where main channel/tidal channel and downriver/upriver were fixed factors in the analysis. We assessed the effect of river discharge on annual increments in surface elevation, surface accretion, and shallow subsidence using analysis of covariance (ANCOVA). River discharge, rainfall, and turbidity were highly correlated (Fig. 2) and thus we used annual river discharge data in these analyses. In our analyses, annual mean river discharge was considered independent, as it was not significantly correlated with time (years).

Results

Monitoring over years

Surface elevation was variable over years, with few sites showing strong linear trends over time (Fig. 3; Table 2). Change in surface elevation between the first and last years of monitoring (over 8 yr) varied between −30 and +80 mm (Fig. 3). Eight of the SET stations had positive trajectories, and four were negative, with an overall mean increase in surface elevation of 1.7 mm per yr^{-1} (standard error ± 1.1, $N = 12$). Variability in surface elevation over time tended to be greater in the main channel sites compared to those in the tidal channel, with a large peak in 2019 at the downriver sites and high levels of variation in the upriver site in the main channel in 2020 (Fig. 3).

There was no significant difference in ΔSurface elevation between the main channel and tidal channel sites ($P > 0.05$), but sites downriver tended to have higher mean ΔSurface elevation than those upriver (Table 2; downriver/upriver $F_{1,8} = 2.82$; $P = 0.131$). For the sites on the tidal channel, there were higher rates of ΔSurface elevation in the downriver position (5.7 mm yr^{-1}) while the mean trends in the upriver position were neutral to negative (− 0.5 mm yr^{-1}) (Table 2).

ΔSurface accretion was also variable, particularly in mangrove sites in the main river channel (Fig. 3; Table 2). While the mean of ΔSurface accretion over all sites was 4.1 ± 1.2 mm per yr^{-1} (N = 12), sites in the main river channel had significantly higher ΔSurface accretion than those in the tidal channel of the South Arm ($F_{1,8} = 63.4$; $P < 0.0001$), and downriver sites had higher rates of ΔSurface accretion than upriver sites ($F_{1,8} = 338$; $P < 0.0001$) (Table 2).

Measurement of changes in the volume of the root zone (in the top 35 cm of soil using ΔPin height) indicated expansion in the root zone of sites in the main channel and neutral to loss of volume (compaction) in sites in the tidal channel of the South Arm ($F_{1,7} = 19.03$; $P = 0.0003$) (Table 2). Changes in root zone volume indicated by ΔPin height were greater in the downriver sites than in the upriver sites ($F_{1,7} = 28.3$; $P = 0.0011$) (Table 2).

Changes in surface elevation can be attributed to surface accretion (material accreted on the soil surface) or to processes within the soil profile, assessed here as ΔShallow subsidence$_{BM}$. Mean ΔShallow subsidence$_{BM}$ was greater in the mangroves fringing the main river channel than in the tidal channel of the South Arm (Table 3; $F_{1,8} = 5.98$; $P = 0.040$). There was no significant effect of downriver/upriver position on ΔShallow subsidence$_{BM}$. We also estimated rates of shallow subsidence in the top 35 cm of the soil profile (ΔShallow subsidence$_{35cm}$) and found that sites in the main channel tended to have lower ΔShallow subsidence$_{35cm}$ compared to sites in the tidal channel of the South Arm, although they were not significantly different ($P > 0.05$). Comparison of mean ΔShallow subsidence$_{BM}$ and ΔShallow subsidence$_{35cm}$ provided an estimate of the shallow subsidence in the deeper layers of the sediment (between 35 cm and the benchmark). The deeper soil layers in the main channel had positive values of shallow subsidence (i.e., decreasing volume over time) while the deeper layers in the tidal channel of the South Arm showed negative values, indicating the expansion of the volume of deeper sediment layers ($F_{1,8} = 6.82$; $P = 0.030$).

Root growth, evaluated in 2017–2018, did not differ between sites in the main channel and the tidal channel ($P > 0.05$; Table 3). The overall mean of 0.37 ± 0.03 g dwt bag^{-1} yr^{-1} scales to a production of 161 g dwt m^{-2} yr^{-1} (in the top 20 cm of soil) which may contribute 1.3 mm yr^{-1} (root volume in cm^3 was estimated from dry mass multiplied by 7.83). Thus, root growth may contribute to surface elevation increments but did so similarly in both the main river and tidal channel in 2017–2018.

Annual variation in surface elevation and accretion

Analysis of annual increments in surface elevation, surface accretion, and shallow subsidence$_{BM}$ indicated significant differences among years (Fig. 3; Surface elevation$_{ANNUAL}$ $P = 0.0023$; Surface accretion$_{ANNUAL}$ $P = 0.0019$). The temporal variation in increments in Surface elevation$_{ANNUAL}$ were different between the main channel and tidal channel settings (year × river/tidal channel interaction $F_{6,48} = 5.16$, $P = 0.004$). For example, high levels of Surface elevation$_{ANNUAL}$ occurred in the main river channel at the downriver site in 2019 associated with flooding, but other sites did not show this high level of surface elevation$_{ANNUAL}$ in the same year (Fig. 3).

Assessment of the effect of annual variation in river flows (log transformed) on Surface elevation$_{ANNUAL}$ found that along the main channel at the downriver site Surface

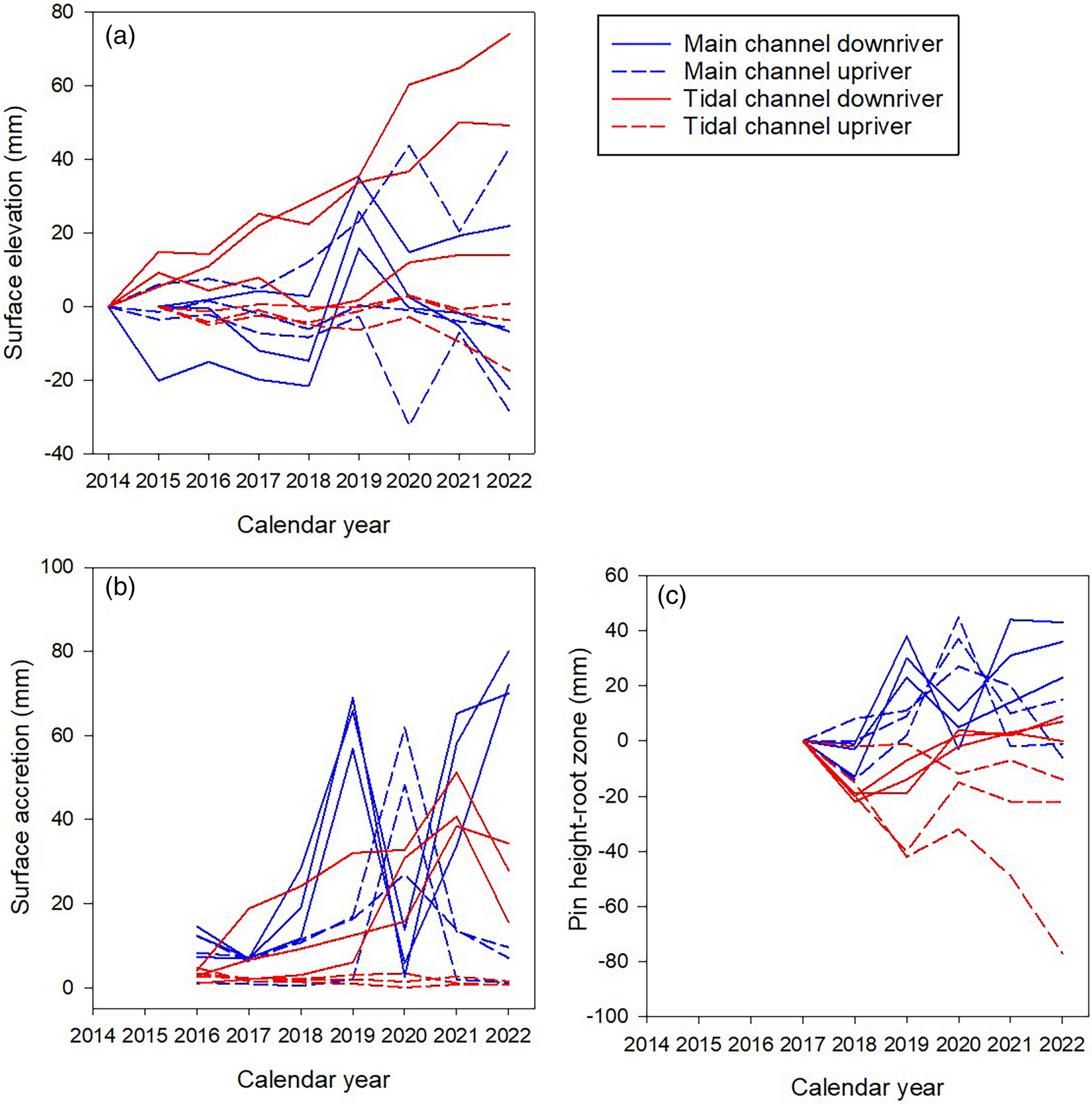

Fig. 3. Temporal trends in surface elevation (**a**), surface accretion (**b**), and volume of the root zone (measured as change in pin height in pins deployed to 35 cm depth) (**c**). Blue lines are for the main channel and red for the tidal channel of the South Arm. Solid lines are for downriver sites and dashed lines are for upriver sites.

elevation$_{\text{ANNUAL}}$ increased with increases in river discharge (Fig. 4; main effect of river discharge $F_{1,71} = 19.83$; $P < 0.0001$). Sites in the tidal channel of the South Arm did not show increases in Surface elevation$_{\text{ANNUAL}}$ with high river discharge. Variation in Surface accretion$_{\text{ANNUAL}}$ followed similar patterns, increasing with levels of river discharge in the main channel, but not in the tidal channel (geomorphic setting × river discharge $F_{1,71} = 17.34$; $P < 0.0001$; Fig. 4). Similarly, Pin height$_{\text{ANNUAL}}$ was influenced by river discharge in the main channel of the river, but not in the tidal channel of the South Arm ($F_{1,40} = 5.09$; $P = 0.0296$), although the relationship was variable (Fig. 4).

Table 2. Results for linear regression of surface elevation, surface accretion, and pin height over years (in mm yr^{-1}) for individual surface elevation table monitoring sites in the Main channel and Tidal channel of the Daintree River, Australia. ΔSurface elevation and ΔSurface accretion were monitored over 8 yr (2013–2022) and ΔPin height over 6 yr (2016–2022). ** indicates $P < 0.05$ and * indicates $P < 0.10$. Mean slope values are ± standard error, $N = 3$. Different letters in the columns indicate means are significantly different.

	ΔSurface elevation			ΔSurface accretion			ΔPin height		
	Slope, mm yr^{-1}	R^2	P	Slope, mm yr^{-1}	R^2	P	Slope, mm yr^{-1}	R^2	P
Main channel									
Downriver1	3.63	0.43	0.046**	9.82	0.47	0.054*	4.22	0.35	0.125
Downriver2	−1.15	0.12	0.64	10.1	0.35	0.095*	8.83	0.36	0.123
Downriver3	1.55	0.01	0.37	8.64	0.37	0.089*	8.37	0.54	0.059*
Downriver mean ± SE	1.3 ± 1.4a			9.5 ± 3.9a			7.1 ± 1.5a		
Upriver1	5.12	0.70	0.003**	2.39	0.11	0.56	0.63	0.24	0.86
Upriver2	−0.55	0.21	0.12	1.77	0.14	0.64	2.11	0.2	0.71
Upriver3	−3.01	0.41	0.036**	0.53	0.17	0.73	3.80	0.09	0.29
Upriver mean ± SE	0.5 ± 2.4a			1.6 ± 0.6b			2.2 ± 0.9a		
Tidal channel									
Downriver1	5.94	0.94	<0.0001**	5.18	0.52	0.040**	2.23	0.03	0.34
Downriver2	1.33	0.29	0.076*	5.32	0.44	0.064*	3.49	0.18	0.22
Downriver3	9.79	0.96	<0.0001**	5.88	0.81	0.004**	3.74	0.17	0.23
Downriver mean ± SE	5.7 ± 2.4a			5.5 ± 0.2c			3.2 ± 0.5a		
Upriver1	−1.85	0.60	0.015**	−0.53	0.46	0.055*	−13.6	0.87	0.004**
Upriver2	0.19	0.01	0.38	−0.18	0.20	0.18	−2.74	0.68	0.028**
Upriver3	0.11	0.15	0.80	−0.27	0.65	0.20	−2.60	0.07	0.46
Upriver mean ± SE	−0.5 ± 0.7a			−0.3 ± 0.1d			−6.3 ± 3.3b		

Discussion

Over the four sites within the Daintree River, we observed a range of ΔSurface elevation from −3.0 mm yr^{-1} (main channel, upriver) to 9.8 mm yr^{-1} (tidal channel, downriver) that did not vary significantly among sites (mean ΔSurface elevation of 1.7 mm yr^{-1}). The local rate of sea level rise in the region is 1.8 mm yr^{-1} (Cairns, Queensland), suggesting that the adjustment of the mangroves of the Daintree River to current rates of sea level rise is variable among sites, similar to observations in surface elevation in other mangroves of Australia (Lovelock et al. 2011; Rogers et al. 2014; Saintilan et al. 2023). The upriver site in the tidal channel tended to have lower ΔSurface elevation than other sites, potentially indicating this site could be more vulnerable to sea level rise (e.g., experience changes in species composition or productivity), although improved knowledge of its elevation relative to sea level (i.e., DEM error is 0.3 m; Table 1) is required to assess vulnerability to

Table 3. Values of shallow subsidence to the depth of the benchmark (ΔShallow $subsidence_{BM}$), within the top 35 cm of soil measured with pins (ΔShallow $Subsidence_{35cm}$) and shallow subsidence in the deeper layers of the soil (ΔShallow $subsidence_{BM\text{-}35cm}$) (values are mean ± standard error, $N = 3$). Positive values of shallow subsidence indicate loss of soil volume while negative values indicate expansion. Mean root growth measured in 2017–2018 (± standard error, $N = 15$) observed using root in-growth bags across the different estuarine settings. Different letters in the columns indicate means are significantly different ($P < 0.05$).

River system	Position	ΔShallow $subsidence_{BM}$, mm yr^{-1}	ΔShallow $subsidence_{35cm}$, mm yr^{-1}	ΔShallow $subsidence_{BM\text{-}35cm}$ (inferred by difference), mm yr^{-1}	Root growth in 2017–2018 (g dwt bag^{-1} yr^{-1})
Main channel,	Downriver	8.2 ± 1.6a	2.3 ± 1.6a	5.8 ± 2.8a	0.3 ± 0.1a
Daintree River	Upriver	1.0 ± 1.9ab	−0.6 ± 1.5a	1.7 ± 3.3ab	0.4 ± 0.1b
Tidal channel,	Downriver	0.1 ± 2.6ab	2.3 ± 0.3a	−2.2 ± 2.8ab	0.4 ± 0.1b
south arm	Upriver	0.2 ± 0.6b	6.0 ± 3.5a	−5.8 ± 3.0b	0.3 ± 0.1a

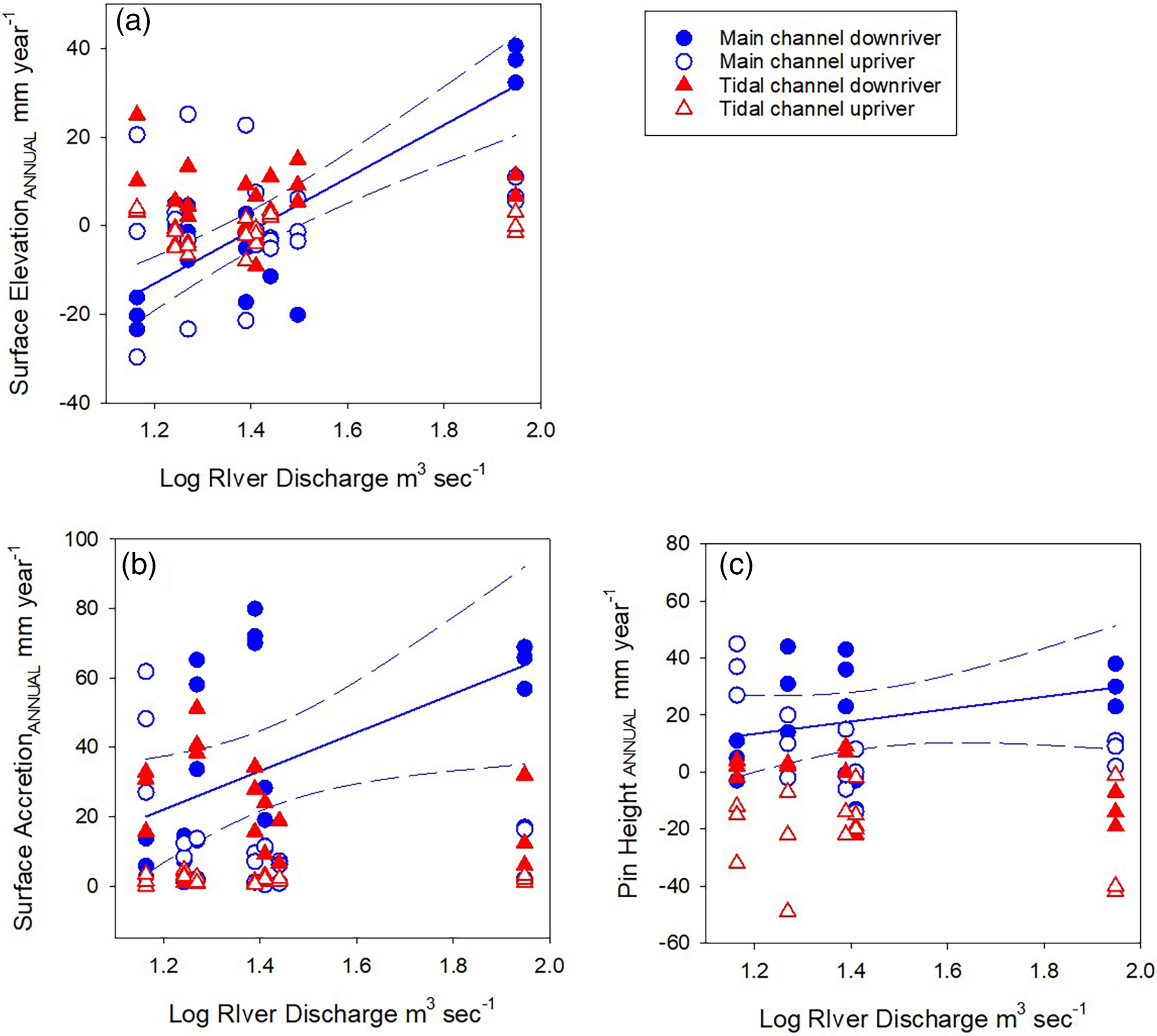

Fig. 4. Relationship between annual river discharge (log transformed, $m^3 sec^{-1}$) and annual increments in surface elevation (**a**), surface accretion (**b**) and pin height (**c**) in mangroves of the Daintree River, Queensland, Australia. Sites in the main channel downriver showed significantly enhanced values with higher levels of river discharge. The line of best fit is shown for the main channel downriver where (a) Surface $elevation_{ANNUAL}$ (mm yr^{-1}) = −84.6 (± 13.2) + 59.7 (± 9.2) * Log(River discharge, m^3 sec^{-1}), $R^2 = 0.66$. (b) Surface $accretion_{ANNUAL}$ (mm yr^{-1}) = −44.6 (± 33.1) + 55.5 (± 23.1) * Log(River discharge, m^3 sec^{-1}), $R^2 = 0.23$; and (c) Pin $height_{ANNUAL}$ (mm yr^{-1}) = −12.6 (± 25.5) + 21.7 (± 17.3) * Log(River discharge, m^3 sec^{-1}), $R^2 = 0.11$. Dashed lines represent the 95% confidence intervals.

sea level rise. Longer time series of surface elevation data and further assessment of factors that vary among sites (e.g., elevation relative to AHD, levels of inundation and rates of water flow) are needed to establish trajectories of ΔSurface elevation to evaluate differences among sites in their vulnerability to sea level rise.

The similarity in ΔSurface elevation in fringing mangroves between the main channel and tidal channel settings (Table 2; Fig. 5) was not consistent with our hypotheses or other research (Hensel et al. 1999; Rogers et al. 2014; McLachlan et al. 2020). However, ΔSurface accretion and changes in the volume of the surface soil layer (ΔPin height) were higher in

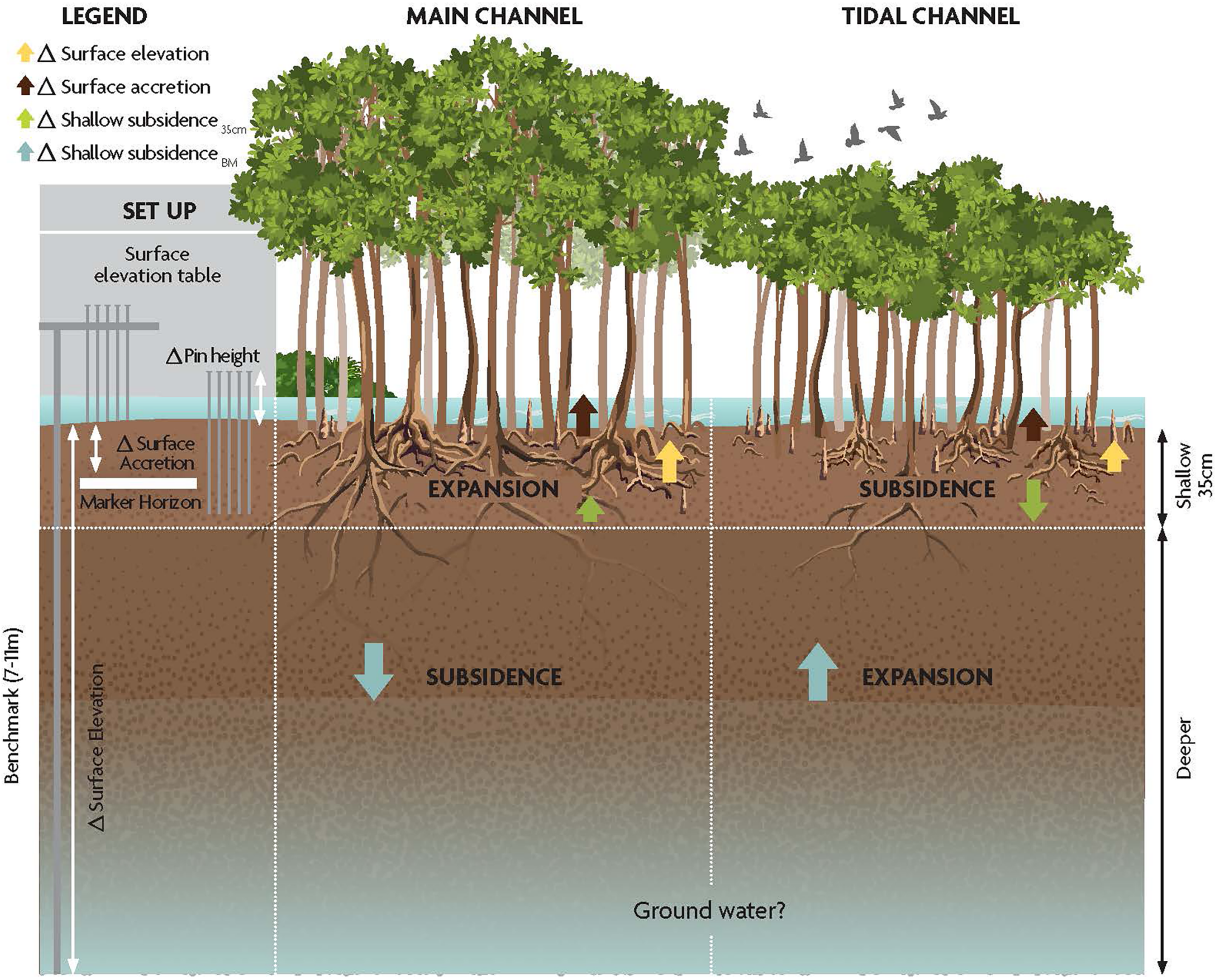

Fig. 5. Summary of the results of this study of comparison between surface elevation, surface accretion, and shallow subsidence to the benchmark and in the top layer of soils in mangrove sites fringing the main river channel (left) and within a tidal channel (right).

the main river channel than in the tidal channel, which was consistent with our hypothesis for a greater role of surface accretion of sediment to surface elevation in the main channel compared to the tidal channel due to higher sediment availability in the main channel of the river (Hensel et al. 1999; McLachlan et al. 2020). Our results are consistent with earlier studies of the Daintree River, where total suspended sediments in the main channel were greatly enhanced in the wet season due to catchment runoff (Davies and Eyre 2005). While there are no studies of variation in turbidity or sediment availability within the tidal channel, turbidity was observed to decline at the junction of the main channel and the tidal channel, suggesting lower availability of sediments to the tidal channel compared to that in the main river channel (Hodge et al. 2005).

ΔSurface accretion and ΔSurface elevation were higher downriver than upriver in both geomorphic settings. In the main river channel, this pattern may arise because of the dispersion of water and sediments over the lower estuary as river flow rates decline, increasing sedimentation in the downriver fringing mangrove (Hoitink et al. 2017; McLachlan et al. 2020). In the tidal channel, downriver sites are closer to the sediment source of the main river channel compared to upriver sites, which may also contribute to high levels of ΔSurface accretion downriver in the tidal channel compared to the upriver site.

The observation that higher ΔSurface accretion in the main channel did not result in higher ΔSurface elevation indicated that shallow subsidence was important in reducing ΔSurface elevation in the mangroves, particularly in the main channel (Table 3; Fig. 5). Furthermore, ΔShallow subsidence$_{BM}$ in the main channel appeared to occur in the deeper layers of the soil, while in the tidal channel of the South Arm ΔShallow subsidence was mainly observed in the soil's surface layer, with expansion occurring in the deeper soil layers. Variation in ΔShallow subsidence among sites could be due to differences in the mass loading (overburden) on soils due to variation in inundation among sites (Rogers and Saintilan 2021) that could be related to local variation in hydrology (e.g., depth of channels, convergence of channels, Hoitink et al. 2017) and variation in tree biomass resulting in differences in the compression of the sediment (Rogers and Saintilan 2021). Root growth, which can offset shallow subsidence (McKee 2011; Krauss et al. 2014), was similar among sites for the 1 yr it was assessed and thus may not contribute to differences in shallow subsidence between main channel and tidal channel settings. However, root growth is likely to vary interannually (Arnaud et al. 2023) reflecting interannual variation in tree growth, which in other sites was observed to vary with annual rainfall (Bennion et al. 2024). The characteristics of soils, including pore sizes, their drainage at low tides, compressibility with loading of tides, and rates of organic matter decomposition can also contribute to variation in ΔShallow subsidence (Xiong et al. 2019; Rogers and Saintilan 2021; Saintilan et al. 2022, 2023; McKee 2011) but were not assessed. Finally, variation in levels of shallow groundwater, where lower levels of groundwater may lead to air-filled pore spaces and thus compressibility of the soil profile, may also contribute to ΔShallow subsidence (Cahoon et al. 2011; Whelan et al. 2005). Interpreting shallow subsurface processes from ΔSurface elevation and ΔSurface accretion measurements is challenging without additional data. Further assessments of the influence of variation in inundation, gradients in soil characteristics and groundwater dynamics, root growth, and decomposition on ΔSurface elevation in the mangroves would provide further insights.

Our assessment of annual variation in surface elevation found that the flood event, observed in 2019, had a clear positive influence on the annual increment in surface accretion and surface elevation in the main channel downriver site (Fig. 4). The relationship between annual river discharge and annual increments in surface elevation was non-linear, reflecting much higher sediment availability with flooding events when sediments are stripped from the catchment and from riverbanks and flow toward the sea (Croke et al. 2017; Bartley et al. 2008). The importance of pulsed rainfall and flooding events to increasing surface elevation has also been reported in mangroves in Micronesia (Krauss et al. 2010) and Florida (Feher et al. 2020), and in saltmarshes in California (Thorne et al. 2022). Using annual increments in surface elevation during the 2019 flood, we estimate that the fringing mangroves of the Daintree River estuary (fringing area of ~ 2000 ha, excluding internal mangrove scrub [Held et al. 2003]) may trap between 10,000 and 50, 000 t of sediment per yr^{-1} (assuming a sediment dry bulk density of ~ 0.5 g cm^{-3}). In extreme floods, mangroves could accumulate 200 t ha^{-1} (i.e., 200 ha of tall fringing *R. apiculata* could trap around 40,000 t per event). A similar proportion of the sediments delivered in floods was reported trapped in mangroves in Micronesia (~ 30%, Golbuu et al. 2003; Victor et al. 2006). Changes in the frequency and intensity of rainfall events with climate change and the resultant frequency and intensity of flooding (Zhang et al. 2021; Hague et al. 2022) will influence sediment availability in the estuary and thus surface elevation increments in the fringing mangrove. Further research could assess the interacting roles of flood pulses, land management practices, and landslides on surface elevation increments of mangroves in the region through longitudinal studies or through comparison of annual surface elevation increments among catchments with differing rainfall intensity, land management, and sediment fluxes (McCloskey et al. 2021).

Limitations

Our study encompasses 8 yr of observations, including one major flood event. While this is comparable in length to many SET records (Sasmito et al. 2016; Saintilan et al. 2023), the length of the data series is limited, site conditions varied, and replication was low, and thus future projections of ΔSurface elevation change and mangrove vulnerability to sea level rise are uncertain. Recently, Byrnes et al. (2019) suggested that the SET method was inappropriate for measuring subsidence in deltaic sediments because (1) they consider subsidence a geological process, and (2) there may be down-drag on the rods in deep sedimentary basins. Subsidence due to geological processes is called "deep subsidence" in the SET literature and is not measured by SETs (Cahoon et al. 2020). At our study location, deep subsidence associated with tectonic activity is very low (~ 0.01–0.02 mm yr^{-1}), although deformation of the crust due to variation in aquifer water storage in the region could vary with extreme El Niño or La Niña conditions (up to ~ 1 mm yr^{-1}, Pan et al. 2022). This deep subsidence, occurring below the SET rods, does not influence the surface processes (from the depth of the SET benchmark) measured using SETs (Cahoon et al. 2020). Studies in New Zealand have demonstrated that down-drag on rods (or pins) in sedimentary basins is small (~ 0.03 mm in unconsolidated sediment) and if occurring would result in a small underestimation of ΔShallow subsidence (Cahoon et al. 2020). Monitoring elevation change of the SET benchmark using Global Positioning System (GPS) surveys could confirm rates of deep subsidence or down-drag of rods (Cahoon et al. 2020), although achieving this in sites with mangrove canopies > 20 m tall would be challenging (Leon et al. 2014). Sub-annual monitoring intervals (multiple times per year), greater knowledge of variation among SET sites within geomorphic settings (in site elevation, inundation levels and other unknown environmental and biotic factors, for example, shallow groundwater, rates of water flows, root growth, organic matter decomposition, variation in activity of bioturbating fauna) along with more detailed monitoring of tidal data and turbidity within the main channel and tidal channel would assist in interpreting future surface elevation monitoring results.

Author Contributions

All authors contributed to data collection and edited the manuscript. Catherine E. Lovelock wrote the first draft of the manuscript and analyzed the data.

Acknowledgments

We thank the reviewers for their suggestions to improve the manuscript. We thank Catherine Bone, Anne Ola, Sang Phan, Vicki Bennion, and many others who assisted in the field during this research. This research was supported by Australian Research Council awards FL200100133, DP150104437, and DP180103444 under Department of Environment and Science, Queensland Government permits WITK14819914 and QFN17/015. Open access publishing facilitated by The University of Queensland, as part of the Wiley - The University of Queensland agreement via the Council of Australian University Librarians.

Conflicts of Interest

None declared.

References

Arnaud, M., S. Krause, R. J. Norby, et al. 2023. "Global Mangrove Root Production, its Controls and Roles in the Blue Carbon Budget of Mangroves." *Global Change Biology* 29: 3256–3270. https://doi.org/10.1111/gcb.16701.

Barbier, E. B. 2017. "Marine Ecosystem Services." *Current Biology* 27: R507–R510. https://doi.org/10.1016/j.cub.2017.03.020.

Bartley, R., R. J. Keen, A. A. Hawdon, P. B. Hairsine, M. G. Disher, and A. E. Kinsey-Henderson. 2008. "Bank Erosion and Channel Width Change in a Tropical Catchment." *Earth Surface Processes and Landforms* 33: 2174–2200. https://doi.org/10.1002/esp.1678.

Bartley, R., C. Thompson, J. Croke, et al. 2018. "Insights Into the History and Timing of Post-European Land Use Disturbance on Sedimentation Rates in Catchments Draining to the Great Barrier Reef." *Marine Pollution Bulletin* 131: 530–546. https://doi.org/10.1016/j.marpolbul.2018.04.070.

Bennion, V., J. M. Dwyer, A. J. Twomey, and C. E. Lovelock. 2024. "Decadal Trends in Surface Elevation and Tree Growth in Coastal Wetlands of Moreton Bay, Queensland, Australia." *Estuaries and Coasts* 47: 1955–1971. https://doi.org/10.1007/s12237-024-01325-y.

Boto, K. G., and J. T. Wellington. 1984. "Soil Characteristics and Nutrient Status in a Northern Australian Mangrove Forest." *Estuaries* 7: 61–69. https://doi.org/10.2307/1351957.

Bunt, J. S., W. T. Williams, and N. C. Duke. 1982. "Mangrove Distributions in North-East Australia." *Journal of Biogeography* 9: 111–120. https://doi.org/10.2307/2844696.

Byrnes, M. R., L. D. Britsch, J. L. Berlinghoff, R. Johnson, and S. Khalil. 2019. "Recent Subsidence Rates for Barataria Basin, Louisiana." *Geo-Marine Letters* 39: 265–278. https://doi.org/10.1007/s00367-019-00573-3.

Cahoon, D. R. 2024. "Measuring and Interpreting the Surface and Shallow Subsurface Process Influences on Coastal Wetland Elevation: A Review." *Estuaries and Coasts* 47, no. 7: 1708–1734. https://doi.org/10.1007/s12237-024-01332-z.

Cahoon, D. R., J. C. Lynch, B. Perez, et al. 2002. "High-Precision Measurements of Wetland Sediment Elevation: II. The Rod Surface Elevation Table." *Journal of Sedimentary Research* 72: 734–739. https://doi.org/10.1306/020702720734.

Cahoon, D. R., B. C. Perez, B. D. Segura, and J. C. Lynch. 2011. "Elevation Trends and Shrink–Swell Response of Wetland Soils to Flooding and Drying." *Estuarine, Coastal and Shelf Science* 91: 463–474. https://doi.org/10.1016/j.ecss.2010.03.022.

Cahoon, D. R., D. J. Reed, J. W. Day, J. C. Lynch, A. Swales, and R. R. Lane. 2020. "Applications and Utility of the Surface Elevation Table–Marker Horizon Method for Measuring Wetland Elevation and Shallow Soil Subsidence-Expansion: Discussion/reply to: Byrnes M., Britsch L., Berlinghoff J., Johnson R., and S. Khalil. 2019. Recent subsidence rates for Barataria Basin, Louisiana. Geo-Marine Letters 39: 265–278." *Geo-Marine Letters* 40: 809–815. https://doi.org/10.1007/s00367-020-00656-6.

Castañeda-Moya, E., R. R. Twilley, V. H. Rivera-Monroy, B. D. Marx, C. Coronado-Molina, and S. M. Ewe. 2011. "Patterns of Root Dynamics in Mangrove Forests Along Environmental Gradients in the Florida Coastal Everglades, USA." *Ecosystems* 14: 1178–1195. https://doi.org/10.1007/s10021-011-9473-3.

Croke, J., C. Thompson, and K. Fryirs. 2017. "Prioritising the Placement of Riparian Vegetation to Reduce Flood Risk and End-Of-Catchment Sediment Yields: Important Considerations in Hydrologically-Variable Regions." *Journal of Environmental Management* 190: 9–19. https://doi.org/10.1016/j.jenvman.2016.12.046.

Davies, P. L., and B. D. Eyre. 2005. "Estuarine Modification of Nutrient and Sediment Exports to the Great Barrier Reef Marine Park From the Daintree and Annan River Catchments." *Marine Pollution Bulletin* 51: 174–185. https://doi.org/10.1016/j.marpolbul.2004.11.008.

Duke, N., M. Ball, and , J. Ellison. 1998. Factors influencing biodiversity and distributional gradients in mangroves. *Global Ecology & Biogeography Letters*, 7(1), pp. 27–47.

Feher, L. C., M. J. Osland, G. H. Anderson, et al. 2020. "The Long-Term Effects of Hurricanes Wilma and Irma on Soil Elevation Change in Everglades Mangrove Forests." *Ecosystems* 23: 917–931. https://doi.org/10.1007/s10021-019-00446-x.

Friess, D. A., M. F. Adame, J. B. Adams, and C. E. Lovelock. 2022. "Mangrove Forests Under Climate Change in a 2 C World." *Wiley Interdisciplinary Reviews: Climate Change* 13: e792. https://doi.org/10.1002/wcc.792.

Geoscience Australia. 2015. Geoscience Australia 2015. Digital Elevation Model (DEM) of Australia Derived From LiDAR 5 Metre Grid. Canberra: Geoscience Australia. https://doi.org/10.26186/89644.

Golbuu, Y., S. Victor, E. Wolanski, and R. H. Richmond. 2003. "Trapping of Fine Sediment in a Semi-Enclosed Bay, Palau, Micronesia." *Estuarine, Coastal and Shelf Science* 57: 941–949. https://doi.org/10.1016/S0272-7714(02)00424-9.

Goldberg, L., D. Lagomasino, N. Thomas, and T. Fatoyinbo. 2020. "Global Declines in Human-Driven Mangrove Loss." *Global Change Biology* 26: 5844–5855. https://doi.org/10.1111/gcb.15275.

Hague, B. S., D. A. Jones, D. Jakob, S. McGregor, and R. Reef. 2022. "Australian Coastal Flooding Trends and Forcing Factors." *Earth's Future* 10: e2021EF002483. https://doi.org/10.1029/2021EF002483.

Harris, P. T., A. D. Heap, S. M. Bryce, R. Porter-Smith, D. A. Ryan, and D. T. Heggie. 2002. "Classification of Australian Clastic Coastal Depositional Environments Based Upon a Quantitative Analysis of Wave, Tidal, and River Power." *Journal of Sedimentary Research* 72: 858–870. https://doi.org/10.1306/040902720858.

Held, A., C. Ticehurst, L. Lymburner, and N. Williams. 2003. "High Resolution Mapping of Tropical Mangrove Ecosystems Using Hyperspectral and Radar Remote Sensing." *International Journal of Remote Sensing* 24: 2739–2759. https://doi.org/10.1080/0143116031000066323.

Hensel, P. E., J. W. Day Jr., and D. Pont. 1999. "Wetland Vertical Accretion and Soil Elevation Change in the Rhone River Delta, France: The Importance of Riverine Flooding." *Journal of Coastal Research* 15: 668–681. https://www.jstor.org/stable/4298983.

Hodge, J., B. Longstaff, A. Steven, P. Thornton, P. Ellis, and I. McKelvie. 2005. "Rapid Underway Profiling of Water Quality in Queensland Estuaries." *Marine Pollution Bulletin* 51: 113–118. https://doi.org/10.1016/j.marpolbul.2004.10.043.

Hoitink, A. J. F., Z. B. Wang, B. Vermeulen, Y. Huismans, and K. Kästner. 2017. "Tidal Controls on River Delta Morphology." *Nature Geoscience* 10: 637–645. https://doi.org/10.1038/ngeo3000.

Krauss, K. W., D. R. Cahoon, J. A. Allen, K. C. Ewel, J. C. Lynch, and N. Cormier. 2010. "Surface Elevation Change and Susceptibility of Different Mangrove Zones to Sea Level Rise on Pacific High Islands of Micronesia." *Ecosystems* 13: 129–143. https://doi.org/10.1007/s10021-009-9307-8.

Krauss, K. W., K. L. McKee, C. E. Lovelock, et al. 2014. "How Mangrove Forests Adjust to Rising Sea Level." *New Phytologist* 202: 19–34. https://doi.org/10.1111/nph.12605.

Kroon, F. J., P. M. Kuhnert, B. L. Henderson, et al. 2012. "River Loads of Suspended Solids, Nitrogen, Phosphorus and Herbicides Delivered to the Great Barrier Reef Lagoon." *Marine Pollution Bulletin* 65: 167–181. https://doi.org/10.1016/j.marpolbul.2011.10.018.

Leon, J. X., G. B. Heuvelink, and S. R. Phinn. 2014. "Incorporating DEM Uncertainty in Coastal Inundation Mapping." *PLoS One* 9, no. 9: e108727. https://doi.org/10.1371/journal.pone.0108727.

Leonard, S., and J. Nott. 2015. "Rapid Cycles of Episodic Adjustment: Understanding the Holocene Fluvial Archive of the Daintree River of Northeastern Australia." *Holocene* 25: 1208–1219. https://doi.org/10.1177/0959683615580860.

Lough, J. M. 1994. "Climate Variation and El Nino-Southern Oscillation Events on the Great Barrier Reef: 1958 to 1987." *Coral Reefs* 13: 181–185. https://doi.org/10.1007/BF00301197.

Lovelock, C. E., V. Bennion, A. Grinham, and D. R. Cahoon. 2011. "The Role of Surface and Subsurface Processes in Keeping Pace With Sea Level Rise in Intertidal Wetlands of Moreton Bay, Queensland, Australia." *Ecosystems* 14: 745–757. https://doi.org/10.1007/s10021-011-9443-9.

Lovelock, C. E., R. Reef, and M. C. Ball. 2017. "Isotopic Signatures of Stem Water Reveal Differences in Water Sources Accessed by Mangrove Tree Species." *Hydrobiologia* 803: 133–145. https://doi.org/10.1007/s10750-017-3149-8.

McCloskey, G. L., R. Baheerathan, C. Dougall, et al. 2021. "Modelled Estimates of Fine Sediment and Particulate Nutrients Delivered from the Great Barrier Reef Catchments." *Marine Pollution Bulletin* 165: 112163. https://doi.org/10.1016/j.marpolbul.2021.112163.

McKee, K. L. 2011. "Biophysical Controls on Accretion and Elevation Change in Caribbean Mangrove Ecosystems." *Estuarine, Coastal and Shelf Science* 91: 475–483. https://doi.org/10.1016/j.ecss.2010.05.001.

McKee, K. L., D. R. Cahoon, and I. C. Feller. 2007. "Caribbean Mangroves Adjust to Rising Sea Level Through Biotic Controls on Change in Soil Elevation." *Global Ecology and Biogeography* 16: 545–556. https://doi.org/10.1111/j.1466-8238.2007.00317.x.

McLachlan, R. L., A. S. Ogston, N. E. Asp, A. T. Fricke, C. A. Nittrouer, and V. J. C. Gomes. 2020. "Impacts of Tidal-Channel Connectivity on Transport Asymmetry and Sediment Exchange With Mangrove Forests." *Estuarine, Coastal and Shelf Science* 233: 106524. https://doi.org/10.1016/j.ecss.2019.106524.

Ola, A., S. Schmidt, and C. E. Lovelock. 2018. "The Effect of Heterogeneous Soil Bulk Density on Root Growth of Field-

Grown Mangrove Species." *Plant and Soil* 432: 91–105. https://doi.org/10.1007/s11104-018-3784-5.

Pan, Y., H. Ding, J. Li, et al. 2022. "Transient Hydrology-Induced Elastic Deformation and Land Subsidence in Australia Constrained by Contemporary Geodetic Measurements." *Earth and Planetary Science Letters* 588: 117556. https://doi.org/10.1016/j.epsl.2022.117556.

Rogers, K., and N. Saintilan. 2021. "Processes Influencing Autocompaction Modulate Coastal Wetland Surface Elevation Adjustment with Sea Level Rise." *Frontiers in Marine Science* 8: 694039. https://doi.org/10.3389/fmars.2021.694039.

Rogers, K., N. Saintilan, and C. D. Woodroffe. 2014. "Surface Elevation Change and Vegetation Distribution Dynamics in a Subtropical Coastal Wetland: Implications for Coastal Wetland Response to Climate Change." *Estuarine, Coastal and Shelf Science* 149: 46–56. https://doi.org/10.1016/j.ecss.2014.07.009.

Saintilan, N., N. S. Khan, E. Ashe, et al. 2020. "Thresholds of Mangrove Survival Under Rapid Sea Level Rise." *Science* 368: 1118–1121. https://doi.org/10.1126/science.aba2656.

Saintilan, N., K. E. Kovalenko, G. Guntenspergen, et al. 2022. "Constraints on the Adjustment of Tidal Marshes to Accelerating Sea Level Rise." *Science* 377: 523–527. https://doi.org/10.1126/science.abo7872.

Saintilan, N., Y. Sun, C. E. Lovelock, et al. 2023. "Vertical Accretion Trends in Australian Tidal Wetlands." *Estuaries and Coasts* 47: 2057–2070. https://doi.org/10.1007/s12237-023-01267-x.

Sasmito, S. D., D. Murdiyarso, D. A. Friess, and S. Kurnianto. 2016. "Can Mangroves Keep Pace With Contemporary Sea Level Rise? A Global Data Review." *Wetlands Ecology and Management* 24: 263–278. https://doi.org/10.1007/s11273-015-9466-7.

Sharmila, S., and H. H. Hendon. 2020. "Mechanisms of Multiyear Variations of Northern Australia Wet-Season Rainfall." *Scientific Reports* 10: 5086. https://doi.org/10.1038/s41598-020-61482-5.

Swales, A., and C. E., Lovelock. 2020. Comparison of sediment-plate methods to measure accretion rates in an estuarine mangrove forest (New Zealand). *Estuarine, Coastal and Shelf Science*, 236, p.106642.

Thorne, K., S. Jones, C. Freeman, K. Buffington, C. Janousek, and G. Guntenspergen. 2022. "Atmospheric River Storm Flooding Influences Tidal Marsh Elevation Building Processes." *Journal of Geophysical Research: Biogeosciences* 127, no. 3: e2021JG006592. https://doi.org/10.1029/2021JG006592.

Victor, S., L. Neth, Y. Golbuu, E. Wolanski, and R. H. Richmond. 2006. "Sedimentation in Mangroves and Coral Reefs in a Wet Tropical Island, Pohnpei, Micronesia." *Estuarine, Coastal and Shelf Science* 66: 409–416. https://doi.org/10.1016/j.ecss.2005.07.025.

Whelan, K. R., T. J. Smith, D. R. Cahoon, J. C. Lynch, and G. H. Anderson. 2005. "Groundwater Control of Mangrove Surface Elevation: Shrink and Swell Varies With Soil Depth." *Estuaries* 28: 833–843. https://doi.org/10.1007/BF02696013.

Woodroffe, C. D., K. Rogers, K. L. McKee, C. E. Lovelock, I. A. Mendelssohn, and N. Saintilan. 2016. "Mangrove Sedimentation and Response to Relative Sea Level Rise." *Annual Review of Marine Science* 8: 243–266. https://doi.org/10.1146/annurev-marine-122414-034025.

Xiong, Y., A. Ola, S. M. Phan, J. Wu, and C. E. Lovelock. 2019. "Soil Structure and its Relationship to Shallow Soil Subsidence in Coastal Wetlands." *Estuaries and Coasts* 42: 2114–2123. https://doi.org/10.1007/s12237-019-00659-2.

Zhang, W., K. Furtado, P. Wu, et al. 2021. "Increasing Precipitation Variability on Daily-To-Multiyear Time Scales in a Warmer World." *Science Advances* 7: eabf8021. https://doi.org/10.1126/sciadv.abj9066.

Submitted 10 July 2024
Revised 01 February 2025
Accepted 01 March 2025